Malaysian Journal of Science **27** (2): 123 – 130 (2008)

Variational Calculations of Highly Excited Rovibrational States for the Ground Electronic State of N_2O

Mohammad Noh Daud[1*] and **Gabriel G. Balint-Kurti**[2#]

[1] Department of Chemistry, Faculty of Science, University of Malaya, 50603 Kuala Lumpur, Malaysia
* mnoh@um.edu.my (corresponding author)
[2] School of Chemistry, University of Bristol, BS8 1TS Bristol, United Kingdom
gabriel.balint-kurti@bristol.ac.uk
Received 27th March 2008, accepted in revised form 29th July 2008.

ABSTRACT Variational calculations are presented for highly excited vibrational bound states of N_2O using a newly constructed *ab initio* multireference configuration interaction potential energy surface. The calculations are performed using a Jacobi coordinate system. The vibrational energies are compared with experimental data and the sources of the discrepancy between them are discussed.

ABSTRAK Pengiraan variasi dipersembahkan untuk keadaan-keadaan getaran teruja tinggi bagi N_2O menggunakan satu permukaan *ab initio* tenaga keupayaan interaksi konfigurasi multirujukan yang baru dibina. Pengiraan dibuat menggunakan satu sistem koordinat Jacobi. Tenaga-tenaga getaran dibandingkan dengan data eksperimen dan sumber-sumber perbezaan antara mereka dibincangkan..

(Variational, multireference configuration interaction, potential energy surface, Jacobi coordinate, rovibrational energy)

INTRODUCTION

The ground electronic state, X^1A', of the N_2O molecule has been extensively studied throughout the years, both theoretically and experimentally. The experimental study of the IR of N_2O molecule has been intensified in the last 20 years. Amiot and Guelachvili [1, 2] have recorded infrared spectrum of this molecule which cover the spectral region up to 8200 cm^{-1} using Fourier Transform spectroscopy. Campargue et al. [3] have completed the analysis of the FT spectrum of N_2O in the near infrared and visible region and have extended it up to 11 000 cm^{-1}. This group has also reported the spectrum for a number of bands of N_2O using intracavity laser spectroscopy between 11 700 and 15 000 cm^{-1}. Various potential energy surfaces have been determined for this state, including empirical fits as those performed by Lacy et al. [4], Kobayashi et al. [5] and Teffo et al. [6], and also the *ab initio* calculation carried out by Martin et al. [7] and Csaszar et al. [8]. Some of these surfaces have been used to investigate the vibrational spectrum of N_2O. Zuniga et al. [9] have considered these issues by performing extensive variational calculations of highly excited state up to 15 000 cm^{-1}. A great variety of curvilinear vibrational coordinates have been used to calculate vibrational energies of N_2O such as Radau and hyperspherical coordinates. With a systematic way of adjusting fitted potential energy functions together with the most sophisticated variational methods employed to calculate vibrational energies, all the reported results give excellent agreement when compared to observed values.

This paper presents the two dimensional variational calculations of highly excited vibrational states of N_2O molecule using the recently derived *ab initio* potential energy surface. The surface is interpolated using the spline method and the quality of the interpolated potential energy surface is checked by comparing the calculated vibrational energies with the experimental frequencies.

THEORY

The quantum mechanical characterisation of a molecular system can be formulated either time-

independently or time-dependently. The time-independent approach is based on the time-independent Schrödinger equation:

$$\hat{H}\Psi = E\Psi$$

where in the current case, $\hat{H}$ is the rovibrational Hamiltonian of the system. The eigenvalues and eigenfunctions of $\hat{H}$ can be obtained using the Rayleigh variational principle which leads to the direct diagonalisation of the Hamiltonian matrix. The resultant eigenvalues provide information on the rovibrational spectrum of the system.

The relevant coordinates employed for the body-fixed (rotating) frame are the Jacobi coordinates (R, r, θ) as depicted in Figure 1. The three Euler angles ($\omega \equiv \alpha, \beta, \gamma$) define the orientation of the body-fixed axes (x, y, z) with respect to the space-fixed (non-rotating) axes (X, Y, Z). The nuclear Hamiltonian operator for a triatomic molecule in the Jacobi coordinates system is expressed as [10, 11]

$$\begin{aligned}\hat{H} = &\left\{-\frac{\hbar^2}{2\mu}\frac{\partial^2}{\partial R^2} - \frac{\hbar^2}{2\mu_r}\frac{\partial^2}{\partial r^2}\right\} \\ &- \left(\frac{\hbar^2}{2\mu R^2} - \frac{\hbar^2}{2\mu_r r^2}\right) \\ &\times \left\{\frac{1}{\sin\theta}\frac{\partial}{\partial\theta}\sin\theta\frac{\partial}{\partial\theta} - \frac{K^2}{\sin^2\theta}\right\} \\ &+ V(R,r,\theta)\Phi^{JK}(R,r,\theta,t) \\ &+ \left(\frac{\hbar^2}{2\mu R^2}\right)\left(J(J+1) - 2K^2\right) \\ &- \frac{\hbar^2 C^{+}_{JK}}{2\mu R^2}\left\{\frac{\partial}{\partial\theta} - K\cot\theta\right\} \\ &- \frac{\hbar^2 C^{-}_{JK}}{2\mu R^2}\left\{-\frac{\partial}{\partial\theta} - K\cot\theta\right\}\end{aligned} \quad \textbf{(1)}$$

where

$$C^{\pm}_{JK} = \left[J(J+1) - K(K\pm 1)\right]^{1/2},$$

V is the electronic potential energy, J is the total angular momentum quantum number, and K is the quantum number for the projections of **J** and of **j** onto the body-fixed z axis. K is the so-called the helicity angular momentum quantum number.

The nuclear wavefunction corresponding to a particular J and M can be expressed in the form of [10, 12, 13]

$$\Psi^{J,M,p}(R,r,\theta,\omega) = \sum_{K=\lambda}^{J}\Phi^{J,K,p}(R,r,\theta) \times |J,K,M,p\rangle \quad \textbf{(2)}$$

where M is the quantum number for the projection of **J** onto the space-fixed Z axis and λ is defined as

$$\lambda = \frac{1-(-1)^{J+p}}{2}. \quad \textbf{(3)}$$

The parity adapted body-fixed angular momentum basis functions in eq. (2) is defined as

$$\begin{aligned}|J,K,M,p\rangle = &\sqrt{\frac{2J+1}{8\pi^2}}\frac{1}{\sqrt{2(1+\delta_{0,K})}} \\ &\times\left[D^{J}_{K,M}(\omega) + (-1)^{J+K+p}D^{J}_{-K,M}(\omega)\right]\end{aligned} \quad \textbf{(4)}$$

where $D^{J}_{K,M}$ indicates the rotation matrix of Wigner D-functions.

$\lambda = K_{\min}$ in eq. (3) takes on the value of 0 or 1, depending on the value of $(-1)^{J+p}$ where $p = 1$ and $p = 2$ correspond to the states of odd parity and even parity, respectively. For $K \neq 0$, p takes on the value of 1 or 2. For $K = 0$, p takes on only the value of 2 because if $J = 0$, the only possible value of λ is 0. For a given J, there exist $2J + 1$ wavefunctions which correspond to different K. The K and $-K$ terms have been grouped together in one parity-adapted wavefunction (see eq. (4)). Therefore, the $2J + 1$ fold degenerate of K states can now be divided into a set of $J + 1$ fold degenerate with $K = 0, 1, 2, 3, \ldots, J$ for even parity states ($p = 2$) and a set of J fold degenerate states with $K = 1, 2, 3, \ldots, J$ for odd parity states ($p = 1$).

Notations of v_1, v_2 and v_3 are used to denote vibrational quanta for the N_2-O stretching, N_2-O bending and N-NO stretching, respectively. The notation of (v_1, $v_2^{|l|}$, v_3) is used for the degenerate states of (v_1, v_2, v_3), distinguished by a vibrational angular momentum l that the allowed values of l are connected with the bending quantum numbers, v_2, by $l = -v_2, -v_2 + 2, \ldots, +v_2$. The allowed values of the total angular momentum quantum number J are connected with l by $J = |l|, |l| + 1, \ldots$. Accordingly, to compute the rotational-vibrational energy and wavefunction for a state with an odd bending quantum number, we considered $J = 1$ with parity state either odd or even. For an odd parity state, the allowed K values are 0 and 1, while for an even parity state the allowed K value is 0. For a state with an even bending quantum number, we considered $J = 0$ with even parity state where $J = 0$ with

odd parity state is symmetry forbidden. Since the total angular momentum, J, and parity are good quantum numbers, the bound state computations were performed separately for different values of J and parity. On the other hand, the helicity quantum number K is not conserved and different values of K were coupled.

A uniform grid was used for the coordinate R and the action of the associated kinetic energy operator on the bound state wavefunction is evaluated using fast Fourier transforms [14, 15]. The radial kinetic energy operator is diagonal in momentum space. For this reason, the wavefunction is transformed to its momentum representation via the fast Fourier transform technique

$$\Phi^{J,K,p}(k_R, r, \theta) = \frac{1}{\sqrt{2\pi}} \int_0^\infty \exp(-ik_R R) \times \Phi^{J,K,p}(R, r, \theta)\, dR$$

$$\Phi^{J,K,p}(R, r, \theta) = \frac{1}{\sqrt{2\pi}} \int_{-\infty}^\infty \exp(ik_R R) \times \Phi^{J,K,p}(k_R, r, \theta)\, dk_R,$$

multiplied by the kinetic energy at the each momentum grid point

$$\left\{-\frac{\hbar^2}{2\mu}\frac{\partial^2}{\partial R^2}\right\}\Phi^{J,K,p}(R, r, \theta)$$
$$= \left\{-\frac{\hbar^2}{2\mu}\frac{\partial^2}{\partial R^2}\right\}\frac{1}{\sqrt{2\pi}}\int_{-\infty}^\infty \exp(ik_R R) \times \Phi^{J,K,p}(k_R, r, \theta)\, dk_R$$
$$= \left\{\frac{\hbar^2}{2\mu}\right\}\frac{1}{\sqrt{2\pi}}\int_{-\infty}^\infty k_R^2 \exp(ik_R R) \times \Phi^{J,K,p}(k_R, r, \theta)\, dk_R$$

and transformed back to the coordinate representation

$$\left\{-\frac{\hbar^2}{2\mu}\frac{\partial^2}{\partial R^2}\right\}\Phi^{J,K,p}(R, r, \theta)$$
$$= \left\{\frac{\hbar^2}{2\mu}\right\}\frac{1}{\sqrt{2\pi}}\int_{-\infty}^\infty k_R^2 \exp(ik_R R) \times \Phi^{J,K,p}(k_R, r, \theta)\, dk_R$$
$$= \left\{\frac{\hbar^2}{2\mu}\right\}\frac{1}{\sqrt{2\pi}}\int_{-\infty}^\infty k_R^2 \exp(ik_R R) \times \frac{1}{\sqrt{2\pi}}\int_0^\infty \exp(-ik_R R') \times \Phi^{J,K,p}(R', r, \theta)\, dR' dk_R.$$

A grid or discrete variable representation (DVR) approach [16] was used to evaluate the action of

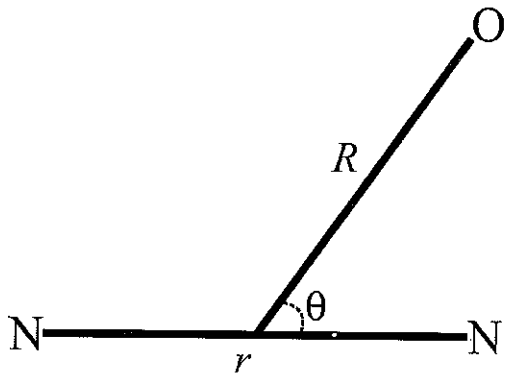

Figure 1. Jacobi coordinates used in the potential energy and dynamics calculations: r denotes the bond distance of the N_2 diatomic; R denotes the bond distance between the centre of mass of N_2 diatomic and O atom; θ denotes the N_2-O Jacobi angle.

The angular part of the kinetic energy operator on the bound state wavefunction, and consequently the angular grid points correspond to Gauss-Legendre quadrature points. In order to perform this operation, we expand the wavefunction in terms of normalised associated Legendre polynomials

$$\Phi^{J,K,p}(R, r, \theta) = \sum_j \Phi_j^{J,K}(R, r)\, \Theta_{jK}(\theta)$$

and use the fact that the associated Legendre polynomials are eigenfunctions of the operator for the first angular term

$$-\left(\frac{\hbar^2}{2\mu R^2} - \frac{\hbar^2}{2\mu_r r^2}\right) \times \left\{\frac{1}{\sin\theta}\frac{\partial}{\partial\theta}\sin\theta\frac{\partial}{\partial\theta} - \frac{K^2}{\sin^2\theta}\right\}\Theta_{jK}(\theta)$$
$$= \hbar^2 j(j+1)\Theta_{jK}(\theta)$$

Corey and Lemoine [17] have discussed how a single set of angular grid points are used in conjunction with the associated Legendre polynomials, corresponding to different K values. The grid representation for the wavefunction is therefore

$$\bar{\Phi}^{J,K}(R_i, r_j, \theta_\alpha) = \sqrt{w_\alpha}\Phi^{J,K}(R_i, r_j, \theta_\alpha)$$

where $w_\alpha = \sin\theta_\alpha$ are the Gauss-Legendre weights and θ_α are the grid points. The normalised associated Legendre functions constitute our fixed basis representation (FBR). The transformation matrix from the DVR to the FBR representation is given by

$$T_{j\alpha}^K = \sqrt{w_\alpha}\Theta_{jK}(\theta_\alpha)$$

Using these equations, we can write one term in the expansion of the wavefunction in terms of the associated Legendre polynomials as

$$\Phi_j^{J,K}(R_i, r_j)\,\Theta_{jK}(\theta) = \sum_\alpha T_{j\alpha}^K \times \bar{\Phi}^{J,K}(R_i, r_j, \theta_\alpha)$$

Since the potential energy is diagonal in coordinate space, its action on the wavefunction involves just the multiplication of the values of potential with those of wavefunction at the same spatial grid points.

RESULTS AND DISCUSSIONS

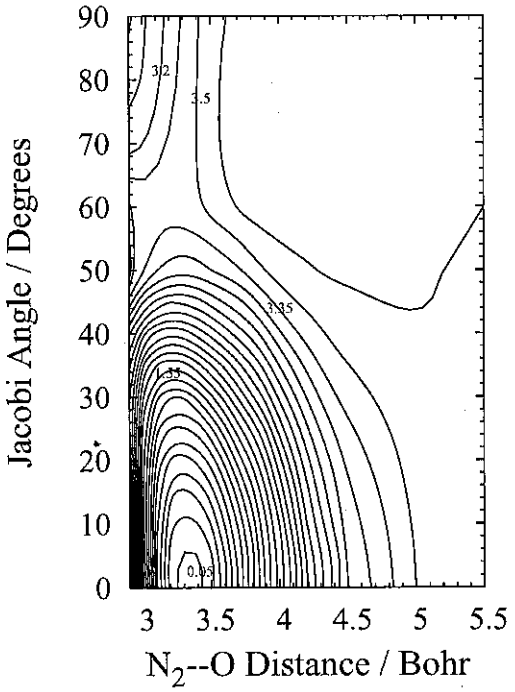

Figure 2. Contour plot of the ground electronic state, $X^1A'(^1\Sigma^+)$, of N_2O at a fixed ground state equilibrium geometry, r_{N-NO} = 2.13199 Bohr. The energies are plotted in eV relative to the minimum of the ground electronic state. The contours spacing are 0.15 eV.

Ab initio calculations of the singlet potential energy surface of the ground electronic state were performed with the MOLPRO package [18] on the Bristol Beowulf cluster systems consisting of two 2.8 GHz Xeon CPUs with 2.0 GB RAM. The final results presented here are produced using the internally contracted multi-reference configuration interaction (MRCI) method including the Davidson correction with an AVQZ basis set [19]. The bulk of the calculations are done using C_s symmetry. The MRCI calculations were preceded by complete active space self consistent field (CASSCF) calculations using an active space that included nine orbitals arising from the $2p$ atomic orbitals of oxygen and nitrogen, respectively. Figure 2 displays a cut through of the potential energy surface of N_2O molecule by fixing one of its internal coordinates at ground state equilibrium geometry.

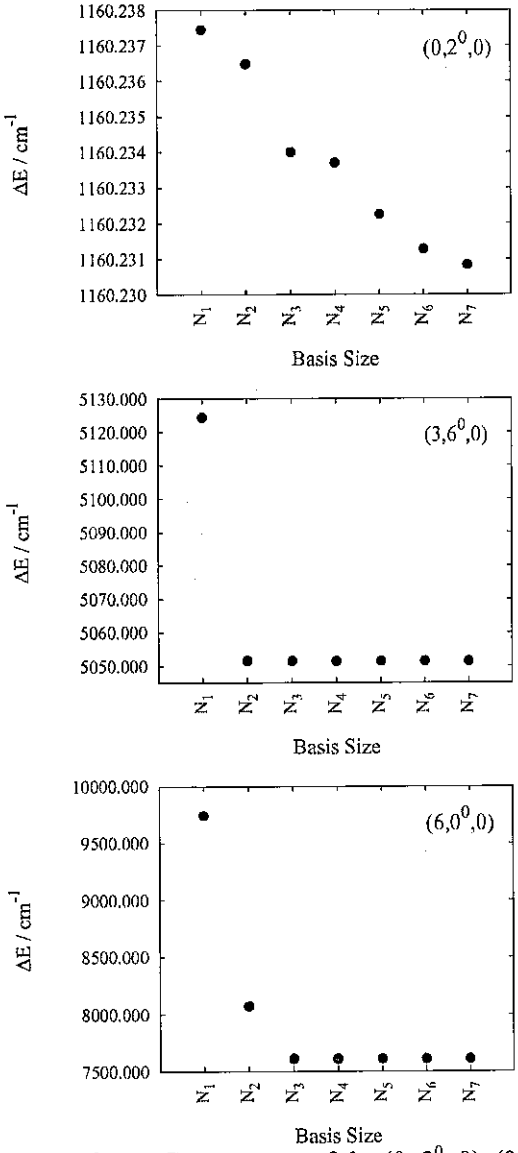

Figure 3. Convergence of the (0, 2^0, 0), (3, 6^0, 0) and (6, 0^0, 0) rotational-vibrational eigenvalues (energies) with the number of the basis functions. N_1, N_2, N_3, N_4, N_5, N_6, and N_7 correspond to the basis functions of n_R = 8 and n_θ = 4, n_R = 12 and n_θ = 6, n_R = 16 and n_θ = 8, n_R = 20 and n_θ = 10, n_R = 22 and n_θ = 12, n_R = 24 and n_θ = 14, and n_R = 26 and n_θ = 16, respectively.

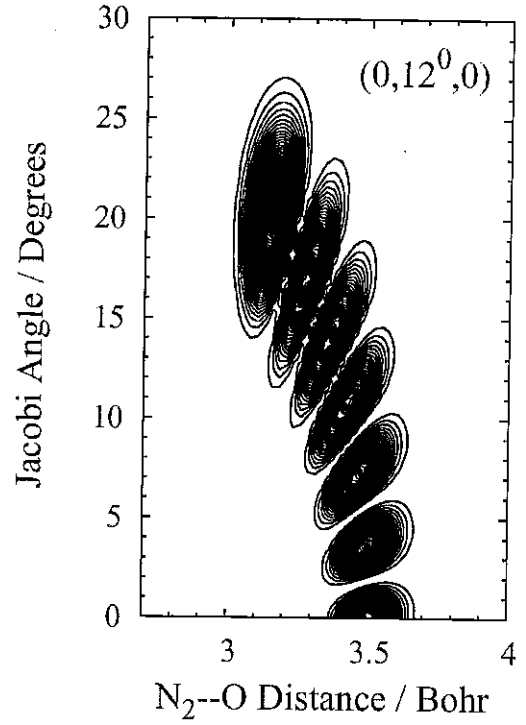

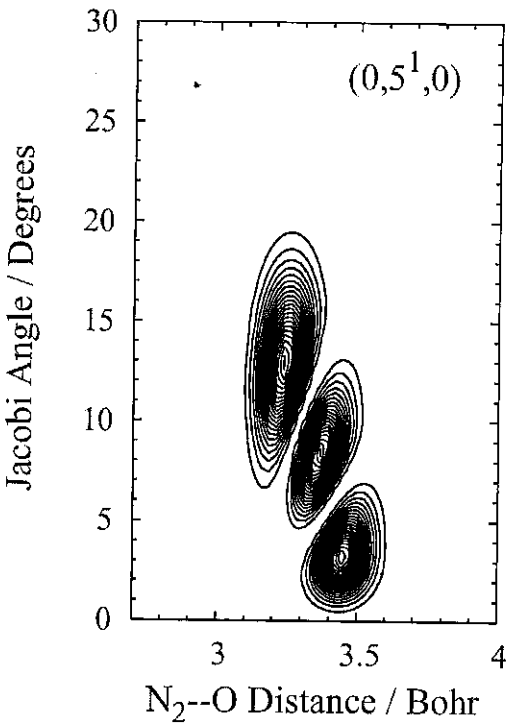

Figure 4. Contour plots of the pure bending vibrational wavefunction for the (0, 12^0, 0) with J = 0 (even parity) and for the (0, 9^1, 0) with J = 1 (odd or even parity)

The dynamics calculations were performed on the personal computer consisting of 2.4 GHz Intel Pentium Core 2 Duo CPU with 2.0 GB

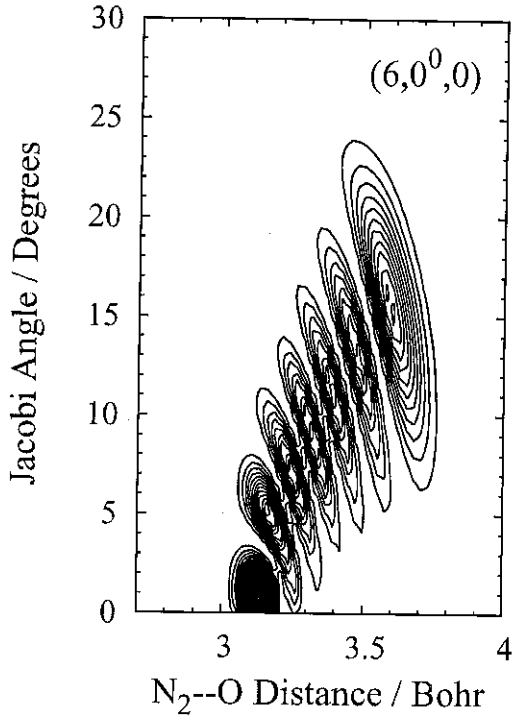

Figure 5. Contour plot of the pure stretching vibrational wavefunction for the (6, 0^0, 0) with J = 0 (even parity)

RAM. There were 64 angular grid points and 384 radial grid points used in the current work. The radial (n_R) and angular (n_θ) basis functions used consisted of 26 number of terms in Legendre polynomials and 16 number of terms in momentum representation, respectively. With the size of basis functions and grid points, the computed two-dimensional vibrational energies were tested for convergence which has been found to converge up to third decimal places. Figure 3(a) shows that by fixing the grid point at 64 and 384, the (0, 2^0, 0) vibrational energy converges from 1160.231281 cm^{-1} to 1160.230832 cm^{-1} as the basis functions increases from n_R = 24 and n_θ = 14 (N_6) to n_R = 26 and n_θ = 16 (N_7). Figure 3(b) show that the (3, 2^0, 0) vibrational energy level converges from 5051.447847 cm^{-1} (N_6) to 5051.447676 cm^{-1} (N_7) and (6, 0^0, 0) vibrational energy level converges from 7611.300399 cm^{-1} (N_6) to 7611.299804 cm^{-1} (N_7). Also observable in Figure 3, the lower vibrational energy of (0, 2^0, 0) state converges much faster than the higher vibrational state. By using a small basis set size of n_R = 8 and n_θ = 4, the (0, 2^0, 0) vibrational energy shows a sufficiently converged value. The assignments of the states were made by visual inspection of the vibrational

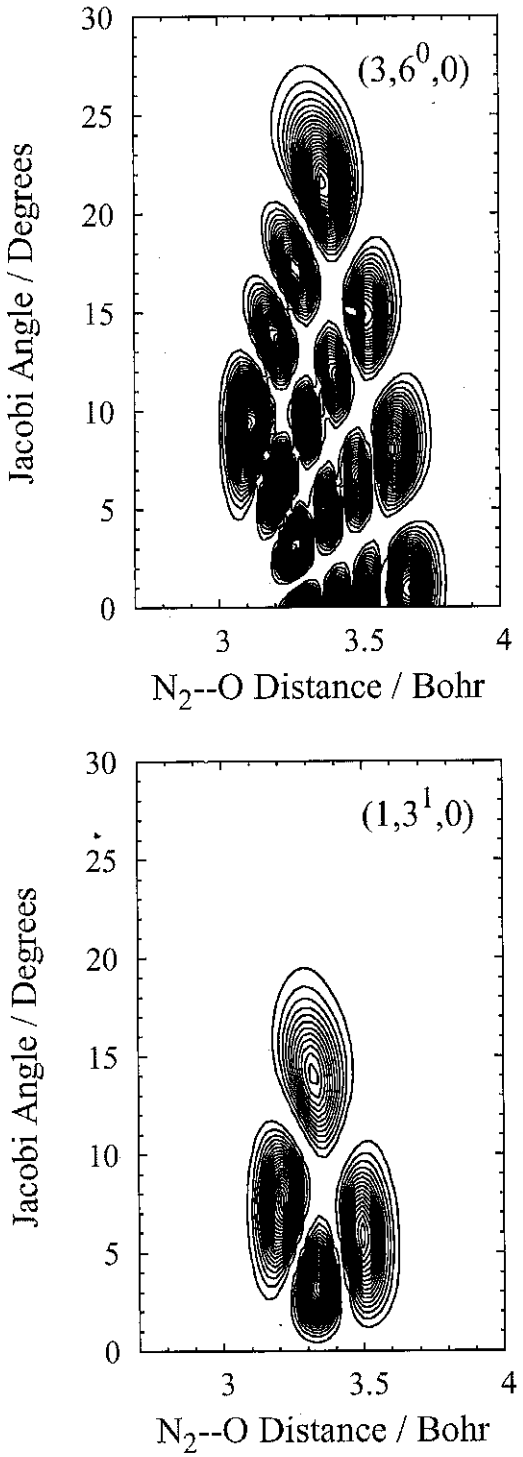

Figure 6. Contour plots of the coupled bending-stretching vibrational wavefunction for the (3, 6^0, 0) with $J = 0$ (even parity) and for the (2, 5^1, 0) with $J = 1$(odd or even parity)

wavefunctions. As examples we show in Figures 4, 5 and 6, the wavefunction contour plots corresponding to the pure bending vibrational mode, pure stretching vibrational mode and coupled bending-stretching vibrational mode, with one of the internal coordinates kept fixed at its equilibrium value.

Table 1. Comparison between calculated and experimental vibrational energies (cm^{-1}) for the X^1A' ground state of N_2O with total angular momentum, $J = 0$ (even parity)

$v_1, v_2^{\lvert l \rvert}, v_3$	ΔE(Theory)[a]	ΔE(Experimental)[b]
0, 0^0, 0	0.00	0.00
0, 2^0, 0	1160.23	1168.13
1, 0^0, 0	1269.77	1284.90
0, 4^0, 0	2315.35	2322.57
1, 2^0, 0	2471.86	2462.00
2, 0^0, 0	2567.08	2563.34
0, 6^0, 0	3450.87	3466.60
1, 4^0, 0	3638.51	3620.94
2, 2^0, 0	3775.57	3748.25
3, 0^0, 0	3857.27	3836.37
0, 8^0, 0	4589.72	
1, 6^0, 0	4782.02	4767.14
2, 4^0, 0	4950.45	4910.99
3, 2^0, 0	5051.45	5026.30
4, 0^0, 0	5130.24	5105.68
0, 10^0, 0	5725.79	
1, 8^0, 0	5936.26	
2, 6^0, 0	6089.22	
3, 4^0, 0	6213.76	6192.27
4, 2^0, 0	6291.10	6295.45
5, 0^0, 0	6377.79	6373.31
0, 12^0, 0	6855.44	
1, 10^0, 0	7068.38	
2, 8^0, 0	7221.43	
3, 6^0, 0	7335.22	
4, 4^0, 0	7433.93	7463.96
5, 2^0, 0	7504.32	7556.11
6, 0^0, 0	7611.30	7640.45

[a] $\Delta E(\text{Theory}) = E(v_1, v_2, v_3) - E(0, 0^0, 0)$

[b] The experimental values were taken from references [1, 2, 3, 20, 21]

In Table 1 and 2 we compare the calculated values for vibrational energies with those observed experimentally. The tables show the energies corresponding to the states with $J = 0$ and $J = 1$, respectively. The first observation is that the agreement between the two sets of results is quite good for some modes while less satisfactory for others, with the maximum discrepancy occurring for the states (5, 2^0, 0), with 39.46 cm^{-1}, and the minimum discrepancy occurring for the states (2, 0^0, 0), with 3.74 cm^{-1}. For those theoretical values that can be compared with the experimental results, the

root-mean-square deviations is 21.98 cm^{-1} for the 28 vibrational energy levels arising from N_2O molecules with $J = 0$ and $J = 1$.

Table 2. Comparison between calculated and experimental vibrational energies (cm^{-1}) for the X^1A' ground state of N_2O with total angular momentum, $J = 1$ (even or odd parity).

$v_1, v_2^{\|l\|}, v_3$	ΔE(Theory)[a]	ΔE(Experimental)[b]
$0, 1^1, 0$	583.67	588.77
$0, 3^1, 0$	1728.10	1749.07
$1, 1^1, 0$	1894.98	1880.27
$0, 5^1, 0$	2885.45	2897.81
$1, 3^1, 0$	3053.09	3046.21
$2, 1^1, 0$	3191.50	3165.86
$0, 7^1, 0$	4022.55	
$1, 5^1, 0$	4207.96	4197.96
$2, 3^1, 0$	4368.04	4335.80
$3, 1^1, 0$	4474.85	4446.38
$0, 9^1, 0$	5051.44	
$1, 7^1, 0$	5164.61	
$2, 5^1, 0$	5360.15	

[a] $\Delta E(\text{Theory}) = E(v_1, v_2, v_3) - E(0, 0^0, 0)$

[b] The experimental values were taken from references [1, 2, 3, 20, 21].

The first and second vibrational excited states in the current two-dimensional case can be assigned to excitation of the pure bending motion, $(0, 1^1, 0)$ and $(0, 2^0, 0)$. The differences of these transition energies with the experimental values are 5.1 cm^{-1} and 7.9 cm^{-1}, respectively, showing that for these motions the coupling between θ and r is of little important. This is supported by the fact that the seventh excitation belongs to the stretching normal mode of the $(1, 0^0, 0)$ state, as previously reported by several workers in the experimental measurements and in the three-dimensional calculations. Therefore, we can expect that the coupling between θ and r is negligibly small at least for the two lowest pure bending vibrations of the ground electronic state of N_2O. For higher pure bending vibrations, they show significant discrepancies with the experimental values, for instance, the maximum discrepancy comes from the state $(0, 3^0, 0)$ which differs by 20.97 cm^{-1}. This is a significant difference, resulting from the coupling of r and θ in the kinetic energy operator and the coupling need to be considered in the calculation.

The third excitation belongs to the motion along R (ΔE = 1269.77 cm^{-1}) which is the stretching normal mode of $(1, 0^0, 0)$ state. There is a significant difference with the experimental normal mode frequency, with the calculated value underestimated by 15.13 cm^{-1}. As observed, the greatest difference comes from the state $(4, 0^0, 0)$, with 21.49 cm^{-1}. The first coupled stretching and bending excitation corresponds to the $(1, 1^1, 0)$ state and its vibrational energy differs by 14.71 cm^{-1} from that of the observed value. The maximum discrepancy comes from the states $(5, 2^0, 0)$ which is also the source of the greatest error in the theoretical calculations.

CONCLUSION

In general, the agreement between the computed and the experimental values is good for low vibrational energies. Nevertheless, at any rate it becomes apparent from these results that a three-dimensional treatment of the vibrational energy level calculations for N_2O is needed for higher vibrational excitations in which anharmonicity and the coupling between the different motions cannot be neglected. Such a computation would require an order of magnitude more computational facilities than were used here. This aspect will be considered in our future work. Due to the fact that the vibration of the N-NO bond is expected to play only a minor role in the photolysis process, it is enough to consider only two-dimensional treatment in the calculations. This assumption is supported from previous experimental finding that at room temperature, the first ultraviolet absorption band arises from excitations starting from the three lowest vibrational energy levels of ground electronic state and the population of these levels accounts for more than 99% of the N_2O ground state vibrational population.

ACKNOWLEDGEMENTS

We thank the University of Malaya for a grant which provided the computational facilities on which these calculations were carried out. We thank to Professor Kurunathan Ratnavelu for his valuable comments.

REFERENCES

1. Amiot, C. and Guelachvili, G. (1974). Vibration-rotation bands of $^{14}N_2{}^{16}O$: 1.2 micron - 3.3 micron region. *J. Mol. Spectrosc.* **51**: 475.

2. Amiot, C. and Guelachvili, G. (1976). Extension of the 10^6 samples Fourier spectrometry to the Indium Antimonide region: Vibration-rotation bands of $^{14}N_2{}^{16}O$: 3.3-5.5 μm region. *J. Mol. Spectrosc.* **59**: 171.
3. Campargue, A., Permogorov, D., Bach, M., Temsamani, M., Auwera, J. V. and Fujii, M. (1995). Overtone spectroscopy in nitrous oxide. *J. Chem. Phys.* **103**: 5931.
4. Lacy, M. and Whiffen, D. H. (1982). The anharmonic force field of nitrous oxide. *Mol. Phys.* **45**: 241.
5. Kobayashi, M. and Suzuki, I. (1987). Sextic force field of nitrous oxide. *J. Mol. Spectrosc.* **125**: 24.
6. Teffo, J. L. and Chedin, A. (1989). Internuclear potential and equilibrium structure of the nitrous oxide molecule from rovibrational data. *J. Mol. Spectrosc.* **135**: 389.
7. Martin, J. M. L., Taylor, P. R. and Lee, T. J. (1993). Accurate ab initio quartic force fields for the N_2O and CO_2 molecules. *Chem. Phys. Lett.* **205**: 535.
8. Csaszar, A. G. (1994). Anharmonic Force Field of N_2O. *J. Phys. Chem.* **98**: 8823.
9. Zúñiga, J., Alacid, M., Bastida, A., Carvajal, F. J. and Requena, A. (1999). Determination of highly excited rovibrational states for N_2O using generalized internal coordinates. *J. Chem. Phys.* **110**: 6339.
10. Balint-Kurti, G. G. (2003). Wavepacket theory of photodissociation and reactive scattering. *Adv. Chem. Phys.* **128**: 249.
11. Offer, C. C. and Balint-Kurti, G. G. (1994). Time-dependent quantum mechanical study of the photodissociation of HOCl and DOCl. *J. Chem. Phys.* **101**: 10416.
12. Balint-Kurti, G. G. and Brown, A. (2004). Time-dependent wavepacket calculations for reactive scattering and photodissociation. *Theory of Chemical Reaction Dynamics*, Kluwer Academic Publishers: 149.
13. Balint-Kurti, G. G., Füsti-Molnár, L. and Brown, A. (2001). Photodissociation of DOBr - Time-dependent wavepacket calculations. *Phys. Chem. Chem. Phys.* **3**: 702.
14. Kosloff, R. (1988). Time-dependent quantum-mechanical methods for molecular dynamics. *J. Phys. Chem.* **92**: 2087.
15. Balint-Kurti, G. G., Dixon, R. N. and Marston, C. C. (1992). Grid methods for solving the schrödinger equation and time dependent quantum dynamics of molecular photofragmentation and reactive scattering processes. *Int. Rev. Phys. Chem.* **11**: 317.
16. Light, J. C., Hamilton, I. P. and Lill, V. J. (1985). Generalized discrete variable approximation in quantum mechanics. *J. Chem. Phys.* **82**: 1400.
17. Corey, G. and Lemoine, D. (1992). Pseudospectral method for solving the time-dependent Schrödinger equation in spherical coordinates. *J. Chem. Phys.* **97**: 4115.
18. MOLPRO, a package of *ab initio* programs designed by Werner, H. -J. and Knowles, P. J. version 2002.1, Amos, R. D., Bernhardsson, A., Berning, A., Celani, P., Cooper, D. L., Deegan, M. J. O., Dobbyn, A. J., Eckert, F., Hampel, C., Hetzer, G., Knowles, P. J., Korona, T., Lindh, R., Lloyd, A. W., McNicholas, S. J., Manby, F. R., Meyer, W., Mura, M. E., Nicklass, A., Palmieri, P., Pitzer, R., Rauhut, G., Schütz, M., Schumann, U., Stoll, H., Stone, A. J., Tarroni, R., Thorsteinsson, T. and Werner, H. -J.
19. Dunning, Jr., T. H. (1989). Gaussian basis sets for use in correlated molecular calculations. I. The atoms boron through neon and hydrogen. *J. Chem. Phys.* **90:** 1007.
20. Toth, R. A. (1991). Line-frequency measurements and analysis of N_2O between 900 and 4700 cm^{-1}. *Appl. Opt.* **30**: 5289.
21. Campargue, A. (1996). The near-infrared absorption spectrum of nitrous oxide: analysis of the $5v_3$ and $v_1 + 5v_3$ clusters. *Chem. Phys. Lett.* **259**: 563.